Dynamic Regulation of ME1 Phosphorylation and Acetylation Affects Lipid Metabolism and Colorectal Tumorigenesis

Yahui Zhu,[1,2,7] Li Gu,[1,2,7] Xi Lin,[1,2] Cheng Liu,[1,2] Bingjun Lu,[1,2] Kaisa Cui,[1,2] Feng Zhou,[3,4] Qiu Zhao,[3,4] Edward V. Prochownik,[5] Chengpeng Fan,[6] and Youjun Li[1,2,8,*]

[1]Hubei Key Laboratory of Cell Homeostasis, College of Life Sciences, Wuhan University, Wuhan 430072, China
[2]Medical Research Institute, School of Medicine, Wuhan University, Wuhan 430071, China
[3]Department of Gastroenterology, Zhongnan Hospital of Wuhan University School of Medicine, Wuhan 430071 China
[4]Hubei Clinical Center and Key Laboratory for Intestinal and Colorectal Diseases, Wuhan 430071, China
[5]Division of Hematology/Oncology, Children's Hospital of Pittsburgh of UPMC, The Department of Microbiology and Molecular Genetics, The Pittsburgh Liver Research Center and The Hillman Cancer Center of UPMC, The University of Pittsburgh Medical Center, Pittsburgh, PA 15224, USA
[6]Department of Biochemistry and Molecular Biology, School of Basic Medical Sciences, Wuhan University, Wuhan 430071, China
[7]These authors contributed equally
[8]Lead Contact
*Correspondence: liy7@whu.edu.cn
https://doi.org/10.1016/j.molcel.2019.10.015

SUMMARY

PGAM5 is a mitochondrial serine/threonine phosphatase that regulates multiple metabolic pathways and contributes to tumorigenesis in a poorly understood manner. We show here that PGAM5 inhibition attenuates lipid metabolism and colorectal tumorigenesis in mice. PGAM5-mediated dephosphorylation of malic enzyme 1 (ME1) at S336 allows increased ACAT1-mediated K337 acetylation, leading to ME1 dimerization and activation, both of which are reversed by NEK1 kinase-mediated S336 phosphorylation. SIRT6 deacetylase antagonizes ACAT1 function in a manner that involves mutually exclusive ME1 S336 phosphorylation and K337 acetylation. ME1 also promotes nicotinamide adenine dinucleotide phosphate (NADPH) production, lipogenesis, and colorectal cancers in which ME1 transcripts are upregulated and ME1 protein is hypophosphorylated at S336 and hyperacetylated at K337. PGAM5 and ME1 upregulation occur via direct transcriptional activation mediated by β-catenin/TCF1. Thus, the balance between PGAM5-mediated dephosphorylation of ME1 S336 and ACAT1-mediated acetylation of K337 strongly influences NADPH generation, lipid metabolism, and the susceptibility to colorectal tumorigenesis.

INTRODUCTION

Colorectal cancer (CRC) is the third most common malignant disease and the fourth leading cause of cancer death worldwide (Torre et al., 2015). Altered metabolism is a common hallmark of cancer cells in general, and CRC in particular, given that rapid tumor growth is dependent on changes in aerobic glycolysis, glutaminolysis, and lipid metabolism (Cotte et al., 2018; Hanahan and Weinberg, 2011; Hao et al., 2016). Most tumors display elevated fatty acid (FA) synthesis and show increases in the transcripts and enzymes that encode the enzymes in these pathways (Finicle et al., 2018). Lipogenesis inhibitors are currently undergoing clinical trials for cancer therapy (Makinoshima et al., 2018; Zadra et al., 2019). However, very little is known about the regulation of these enzymes by post-translational modification and how they contribute, if at all, to CRC induction.

Malic enzymes (ME) participate in the reactions that link anabolic and catabolic branches of metabolism. The cytoplasmic form of ME, ME1, provides one source of nicotinamide adenine dinucleotide phosphate (NADPH) that is used for FA synthesis and glutamine production (Dey et al., 2017; Jiang et al., 2013). ME1 supports tumor growth through its participation in various tumor-related signaling pathways, particularly those involving TP53, Myc, and KRAS. For example, in senescent and cancer cells, TP53 inhibits NADPH production and lipogenesis by decreasing ME1 expression via direct binding to ME1 promoter (Jiang et al., 2013). Depletion of ME1 inhibits mutant KRAS and *APC* mutant-driven CRC growth by decreasing NADPH production and lipogenesis (Fernandes et al., 2018; Lu et al., 2018; Shen et al., 2017). NADPH supports redox defenses and reductive biosynthesis in tumor cells (Wen et al., 2015). ME1 thus stands at an important crossroad that links normal and neoplastic proliferation. However, little is known concerning ME1's post-translational regulation.

Cyclic phosphorylation/dephosphorylation and acetylation/deacetylation play critical roles in the regulation of many essential proteins during different cellular processes including metabolism, carcinogenesis, epigenetic modeling, and survival (Robitaille et al., 2013; Shan et al., 2014; Yang et al., 2012). Recent studies have revealed that K321 acetylation of the

pyruvate dehydrogenase A1 (PDHA1) subunit inhibits PDH activity by recruiting the inhibitory PDH kinase 1 (PDK1). Conversely, the stimulatory PDH phosphatase (PDP1) K202 acetylation inhibits PDH function by dissociating its substrate PDHA1, both of which are critical through promoting glycolysis in tumor growth (Fan et al., 2014; Shan et al., 2014). The epidermal growth factor receptor (EGFR) stimulates the activity of acetyl-CoA acetyltransferase (ACAT1) and stimulates tumor growth by phosphorylating the ACAT1 Y407 residue and promoting its tetramerization (Fan et al., 2016). The acetylation and phosphorylation of metabolic enzymes also may affect their stability, as evidenced by the P300/CBP-associated factor (PCAF)-mediated acetylation of cell death-inducing DFFA-like effector C (CIDEC) (Lin et al., 2013; Qian et al., 2017).

PGAM family member 5 (PGAM5) belongs to the phosphoglycerate mutase family, and in contrast to other family members, functions as an atypical serine/threonine protein phosphatase rather than as a phosphoglycerate mutase. PGAM5 is involved in regulating apoptotic and necroptotic pathways as well as mitochondrial turnover by inducing mitophagy after mitochondrial damage (He et al., 2017; Panda et al., 2016; Ramachandran and Jaeschke, 2017; Wang et al., 2012). PGAM5 is also upregulated in hepatocellular carcinoma and promotes its growth (Cheng et al., 2018).

Here, we report that PGAM5 is upregulated in patients with CRC and functions by dephosphorylating ME1 at S336. This lead to a reciprocal increase in ME1 acetylation by ACAT1 at the adjacent K337 residue and increases in ME1's dimerization and enzymatic activity, both of which are necessary to promote colorectal tumorigenesis. In this manner, ME1 S336 phosphorylation and K337 acetylation are shown to be mutually antagonistic. These findings reveal that an important step in the metabolic reprogramming that accompanies CRC tumorigenesis involves the reciprocal PGAM5-mediated dephosphorylation and ACAT1-mediated acetylation of adjacent residues on ME1 that dictate its inherent metabolic activity.

RESULTS

PGAM5 Is Upregulated in CRC

Numerous kinase inhibitors have been used to treat a variety of cancers including CRC (Qi et al., 2018). However, the selective targeting of protein phosphatases remains a relatively underdeveloped area. To study the role of phosphatases in colorectal tumorigenesis and to identify potential therapeutic targets, we first examined the expression of transcripts encoding 324 known phosphatases in 382 CRCs from the TCGA database. The results indicated that 54 phosphatase genes were commonly upregulated in CRCs (1.6-fold threshold) (Figure 1A). We next analyzed the protein expression of these genes in CRCs from the Human Protein Atlas database and found that, in 10 of 12 tumor samples, only PPM1G and PGAM5 were overexpressed (Figure 1A). To demonstrate a functional role for these two phosphatases in CRC, we knocked down their expression in CRC cells and found that depleting PGAM5 significantly inhibited CRC cell growth, whereas depleting PPM1G had no effect (Figures 1B and S1A). Additional studies revealed that CRCs contained the highest levels of PGAM5 RNA and protein among evaluable tumors

(Figures S1B and S1C). A fuller analysis among 33 different tumor types from the TCGA and GTEx datasets showed that PGAM5 transcripts were also upregulated in most other types of cancer (Figure S1D). PGAM5 RNA levels were also upregulated in virtually all tumors from 32 matched normal colorectal and CRC tissues from the TCGA database (Figure S1E). PGAM5 RNA was also highly upregulated in 31 pairs of matched normal:CRC tissues from Wuhan Union Hospital (Figure 1C) and in CRCs from several GSE databases (Figure S1F). Consistently, PGAM5 RNA and protein levels gradually increased in the colon of C57BL/6 mice after azoxymethane/dextran sulfate sodium (AOM/DSS) treatment (Figures 1D and 1E). Finally, PGAM5 was also significantly upregulated in the colon of $Apc^{Min/+}$ mice (Figures 1F and 1G).

We next investigated the effects of PGAM5 modulation on CRC growth. ShRNA-mediated inhibition of PGAM5 significantly retarded in vivo xenograft growth, and this defect could be rescued by the expression of wild-type (WT) PGAM5 but not by a phosphatase-dead H105A mutant (Figures S1G–S1K). These results indicate that PGAM5 is highly expressed in CRC and necessary to sustain optimal levels of tumor growth.

PGAM5 Dephosphorylates ME1 to Enhance ME1 Activity

To better study how PGAM5 contributes to CRC tumorigenesis, we overexpressed PGAM5 in HEK293 cells and then performed coimmunoprecipitation (coIP) studies followed by SDS-PAGE in order to identify key PGAM5-associated proteins. ME1 was identified as one of the most prominent interactors (Figure 2A) and in reciprocal experiments, PGAM5 was identified as a major ME1 interactor (Figure S2A). The endogenous interactions between PGAM5 and ME1 were confirmed by coIP experiments in CRC cells (Figures 2B and S2B). Collectively, these results show that PGAM5 interacts with ME1 in CRC cells.

Because PGAM5 is a phosphatase, we examined the effect of PGAM5 on ME1 phosphorylation in HCT116 cells. PGAM5 inhibition significantly increased ME1 serine phosphorylation, and this defect could be rescued by expressing WT PGAM5 but not the phosphatase-dead H105A mutant (Figure 2C). Finally, PGAM5 promoted ME1 dimerization (Figures S2C and S2D).

ME1 is an important source of NADPH and plays an important role in lipogenesis (Jiang et al., 2013). Therefore, we quantified ME1 activity and lipid metabolism in stable cells and CRC xenografts. The results showed that PGAM5 depletion inhibited ME1 activity, NADPH production, and lipogenesis but had no effect on the activity of the mitochondrial ME isoform, ME2 (Figures 2D, 2E, and S2E–S2K). Depletion of PGAM5 also decreased glycolysis and the extracellular acidification rate (ECAR), which reflects overall glycolytic flux. Further, it also augmented the oxygen consumption rate (OCR), an indirect indicator of mitochondrial oxidative respiration (Figures 2F, S2L, and S2M). Together, these data demonstrate that PGAM5 directly interacts with ME1, promotes its dimerization, and enhances its ability to generate NADPH and promote lipid synthesis.

NEK1 Phosphorylates ME1 at Serine 336 to Inhibit ME1 Activity

To identify the kinase(s) responsible for ME1 phosphorylation, we analyzed the results of mass spectrometry derived from
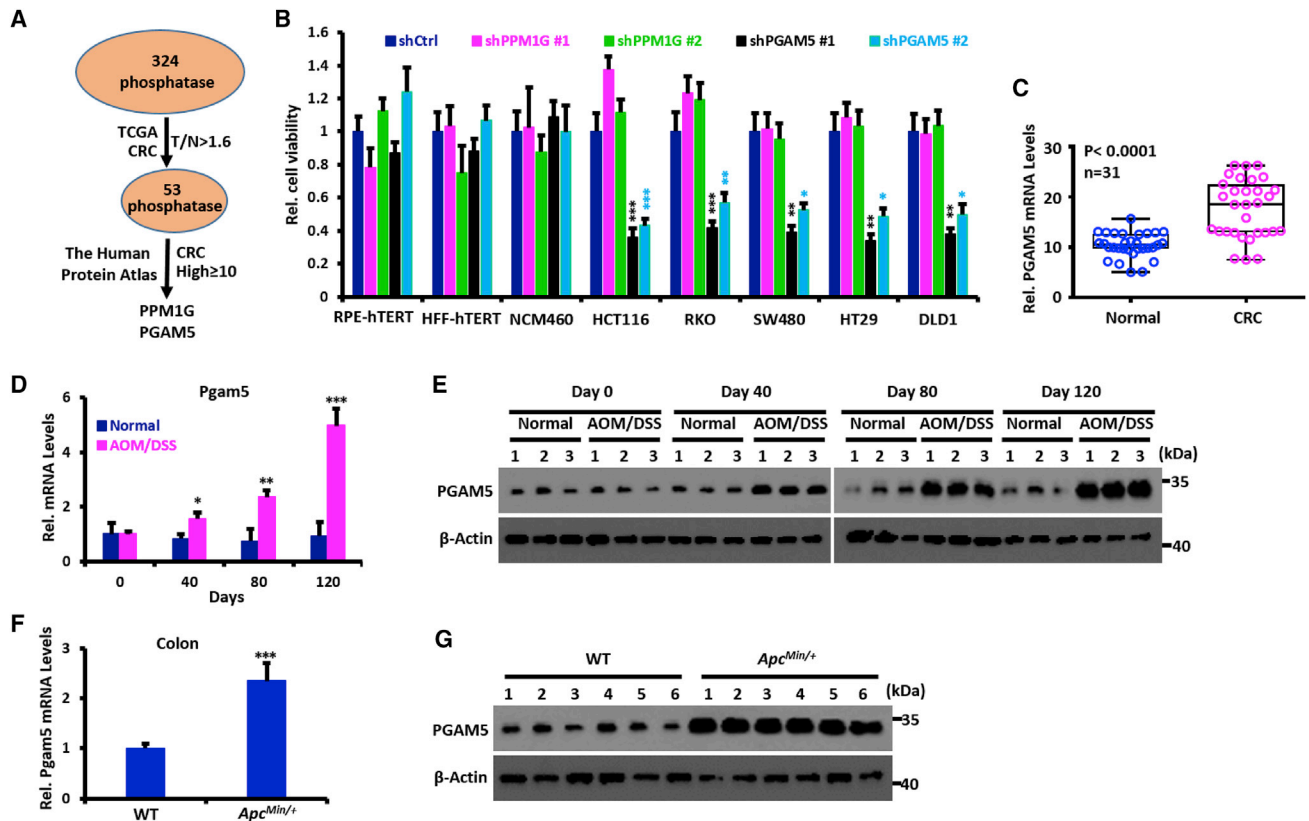
Figure 1. PGAM5 Is Upregulated in CRC

(A) Summary of bioinformatic screening results in CRCs. Among the 324 phosphatase genes examined, 53 were upregulated (tumor/normal >1.6-fold) in CRCs based on transcript levels in the TCGA database. Only PPM1G and PGAM5 protein were highly expressed in 10 of 12 CRC tumors from in The Human Protein Atlas datasets.

(B) MTT assays in CRC cells after transfection with PPM1G and PGAM5 shRNAs.

(C) PGAM5 expression in 31 pairs of CRCs from Wuhan Union Hospital.

(D and E) Relative mRNA (D) and protein (E) levels of PGAM5 during CRC induction with AOM/DSS.

(F and G) Relative mRNA (F) and protein levels (G) of PGAM5 in CRCs from $Apc^{Min/+}$ mice compared with WT mice.

Data were presented as mean ± SD. *$p < 0.05$, **$p < 0.01$, ***$p < 0.001$.

the above-described ME1 IPs and identified 13 peptides derived from NIMA1-related kinase (NEK1) (Figure S2N, left). Interestingly, NEK1 and PGAM5 transcript levels were negatively correlated (Figure S2N, right). CoIP experiments confirmed an association between endogenous ME1 and NEK1 (Figure S2O).

NEK1 depletion drastically decreased ME1 serine phosphorylation. NEK1 depletion could be rescued by the enforced expression of WT NEK1 but not by the T162A mutant (Figure 2G).

To identify the actual serine residue(s) of ME1 phosphorylated by NEK1, we used PhosphoSite Plus to predict candidate phosphorylation sites and mutated these to alanines. We found that NEK1 was unable to phosphorylate the ME1 S336A mutant whereas other mutants were phosphorylated at normal levels (Figure 2H). Consistent with the idea that S336 is the site of NEK1-mediated phosphorylation and PGAM5-mediated dephosphorylation, the co-expression of PGAM5 did not affect the phosphorylated status of the ME1 S336A mutant (Figure S2P). The S336 of ME1 was also found to be highly conserved among different species (Figure S2Q).

To examine the cross-talk between PGAM5 and NEK1 on the serine phosphorylation of ME1, we co-expressed or co-depleted NEK1 and PGAM5 in CRC cells. The studies showed that PGAM5 decreased NEK1-mediated phosphorylation of ME1 whereas NEK1 increased phosphorylation (Figures 2I and S2R). Collectively, these observations demonstrate that ME1 S336 is phosphorylated and dephosphorylated by NEK1 and PGAM5, respectively, and they compete for modification of this site.

ME1 S336 Phosphorylation Abolishes Its Activity

To determine the functional consequences of ME1 S336 phosphorylation, we co-expressed WT ME1 or S336A and S336D mutants with HA- and Flag-tags. CoIP experiments demonstrated that the ME1 S336A mutant was able to efficiently dimerize, whereas S336D was not (Figure S2S). S336A also strongly promoted tumor growth *in vivo* and increased glycolysis, NADPH production, and lipid synthesis in a CRC xenograft, whereas these activities were significantly attenuated in cells expressing S336D (Figures 2J and S2T–S2Z). Together, these data
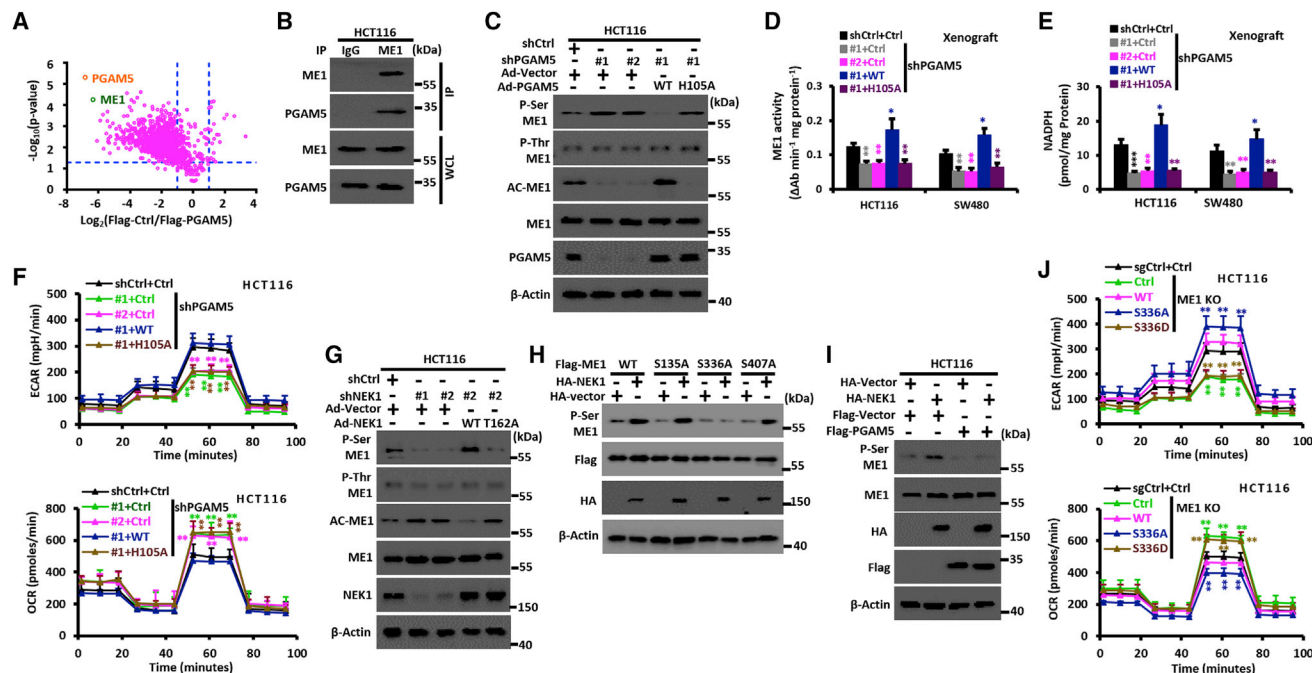
Figure 2. ME1 Is Phosphorylated and Dephosphorylated by NEK1 and PGAM5 at S336, Respectively

(A) Scatterplots displaying comparisons in peptide identities from coIP of control and PGAM5 expressing cells. Cellular extracts from HEK293 cells expressing Flag-PGAM5 or control vector were immuno-purified on anti-Flag affinity columns. The eluates were resolved by SDS-PAGE and Coomassie blue staining. The bands were retrieved and analyzed by mass spectrometry.

(B) Endogenous interaction between PGAM5 and ME1.

(C) Depletion of PGAM5 increases serine phosphorylation of ME1. This is rescued by co-expressing WT PGAM5 but not the H105A mutant.

(D) ME1 activity in xenograft from indicated cells.

(E) NADPH levels in xenograft from indicated cells.

(F) Extracellular acidification rate (ECAR) (top) and oxygen consumption rate (OCR) (bottom) analyses of HTC116 cells from (C). The time at which a given compound was added is indicated.

(G) Depletion of NEK1 reduces serine phosphorylation of ME1. This was rescued with WT NEK1 but not with the inactive T162A mutant.

(H) NEK1 phosphorylates ME1 at S336.

(I) PGAM5 antagonizes NEK1-mediated serine phosphorylation of ME1.

(J) ECAR (top) and OCR (bottom) analyses of HCT116 cells expressing the phosphorylation site mutant of ME1.

Data are presented as mean ± SD. *p < 0.05, **p < 0.01, ***p < 0.001.

demonstrate that ME1 S336 phosphorylation strongly attenuated multiple ME1-mediated activities.

ACAT1 Acetylates ME1 at K337

During the course of our studies, we observed that depleting PGAM5 expression decreased ME1 acetylation while ectopic PGAM5 had the opposite effect (Figure 2C). ME1 acetylation was also increased by depleting NEK1 (Figure 2G). A review of our above-described mass spectrometry analysis of ME1 coIPs identified acetyl CoA transferase (ACAT1) as the most abundant acetyltransferase and thus the most likely ME1 acetylase (Figure S3A). We confirmed both the endogenous interactions between ACAT1 and ME1 (Figures 3A and S3B). Furthermore, depleting ACAT1 expression in CRC cells dramatically decreased ME1 acetylation without affecting its protein level whereas ectopic ACAT1 had the opposite effect (Figure 3B). To determine the impact of ACAT1 on ME1 dimerization, coIP experiments were performed in HEK293 cells stably expressing or depleted for ACAT1. We observed that ectopic ACAT1 expression promoted ME1 dimerization

(Figure S3C) whereas ACAT1 depletion prevented this (Figure S3D).

Five putative acetylation sites of ME1 were predicted in the Protein Lysine Modifications Database. We mutated each individual lysine (K) to an arginine (R) and found that K337R was associated with a significant reduction of ME1 acetylation, indicating that ME1 was likely acetylated at this site (Figure 3C). Ectopic ACAT1 expression proved capable of acetylating all ME1 mutants except K337R (Figure 3C). These data demonstrate that ACAT1 acetylates ME1 at K337, which is also a highly evolutionarily conserved residue (Figure 3D). ME1 K337R showed a marked loss of dimerization potential whereas the acetylation mimetic mutation K337Q demonstrated enhanced dimerization in HCT116 ME1 knockout cells (Figure 3E). Collectively, these results suggest that ACAT1-mediated K337 acetylation positively regulates ME1 dimerization.

ME1 Is Deacetylated by SIRT6 at K337

To identify candidate ME1 deacetylase(s), we used nicotinamide (NAM) and Trichostatin A (TSA) to selectively inhibit members of
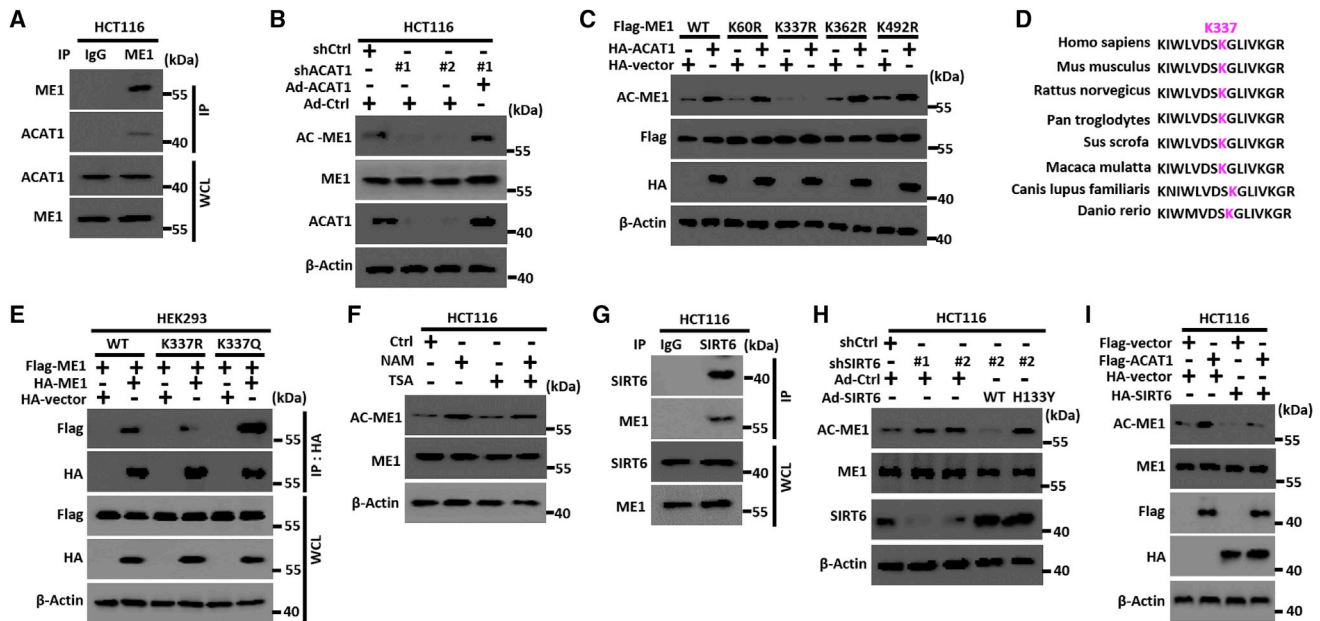
Figure 3. ME1 Is Acetylated and Deacetylated at K337 by ACAT1 and SIRT6, Respectively

(A) Endogenous interactions between ACAT1 and ME1.

(B) ACAT1 inhibition decreases ME1 acetylation.

(C) ACAT1 acetylates ME1 at K337.

(D) Alignment of K337 and adjacent amino acid sequence of ME1 among different species.

(E) ME1 acetylation at K337 enhances its dimerization.

(F) ME1 acetylation is increased by treatment with NAM but not TSA in HCT116.

(G) Interaction between endogenous SIRT6 and ME1.

(H) Depletion of SIRT6 enhances ME1 acetylation in HCT116 cells. Acetylation is reduced by the co-expression of WT SIRT6 but not by the H133Y mutant.

(I) SIRT6 antagonizes ACAT1-mediated ME1 acetylation in HCT116 cells.

the SIRT and HDAC families, respectively. ME1 acetylation dramatically increased in cells treated with NAM, but not TSA (Figure 3F), indicating that a SIRT family member was likely responsible for ME1 deacetylation. To confirm this finding, we co-expressed ME1 and individual members of the SIRT family in HEK293 cells and found that ME1 acetylation was reduced only by SIRT6 (Figure S3E). Endogenous interactions between ME1 and SIRT6 were documented by coIP experiments (Figures 3G and S3F). SIRT6 depletion increased ME1 acetylation (Figure 3H). Ectopic expression of SIRT6 decreased acetylation of WT ME1 and other three mutants, but not K337R mutant (Figure S3G). Taken together, these data indicate that SIRT6 deacetylates ME1 at K337.

To determine the relationship between ACAT1 and SIRT6 on ME1 acetylation, we co-expressed or co-depleted ACAT1 and SIRT6 in CRC cells. The results showed that SIRT6 decreased ACAT1-mediated ME1 acetylation (Figures 3I and S3H).

ME1 S336 Phosphorylation and K337 Acetylation Are Competitively Antagonistic

To better understand the relationship between PGAM5-mediated S336 dephosphorylation and ACAT1-mediated K337 acetylation of ME1 in ME1 KO CRC cells, we expressed WT ME1, S336A, or S336D. The acetylation of ME1 S336A was dramatically enhanced whereas the acetylation of S336D

was reduced (Figure 4A). Conversely, ectopic expression of the ME1 K337R acetylation mutant dramatically enhanced its phosphorylation, whereas ectopic expression of ME1 K337Q, acetylation mimic mutant, had the opposite effect (Figure 4B).

We next determined the role of ACAT1 on the acetylation of ME1 S336A and S336D and the role of NEK1 on phosphorylation of ME1 K337R and K337Q. We found that ACAT1 dramatically enhanced the acetylation of the ME1 S336A, but not S336D (Figure 4C). Similarly, NEK1 co-expression increased the phosphorylation of ME1 K337R but not K337Q (Figure 4D).

We next determined whether ME1's phosphorylation status affected its interaction with ACAT1 and found that ME1 phosphorylation decreased the interaction between ACAT1 and ME1 (Figure 4E). Similarly, ME1 acetylation decreased the interaction between NEK1 and ME1 (Figure 4F). Furthermore, we compared the subcellular localization of ME1 S336A versus S336D and K337R versus K337Q. Subcellular fractionation studies showed ME1 S336D and K337R to be mainly localized to mitochondria, while S336A and K337Q localized mainly to the cytosol (Figure S4A). These data demonstrate that the mechanism by which NEK1 and ACAT1 mutually antagonize one another's activities involves the apparent physical displacement of one protein by the other at their individual substrate recognition residues, namely S336 and K337, respectively.
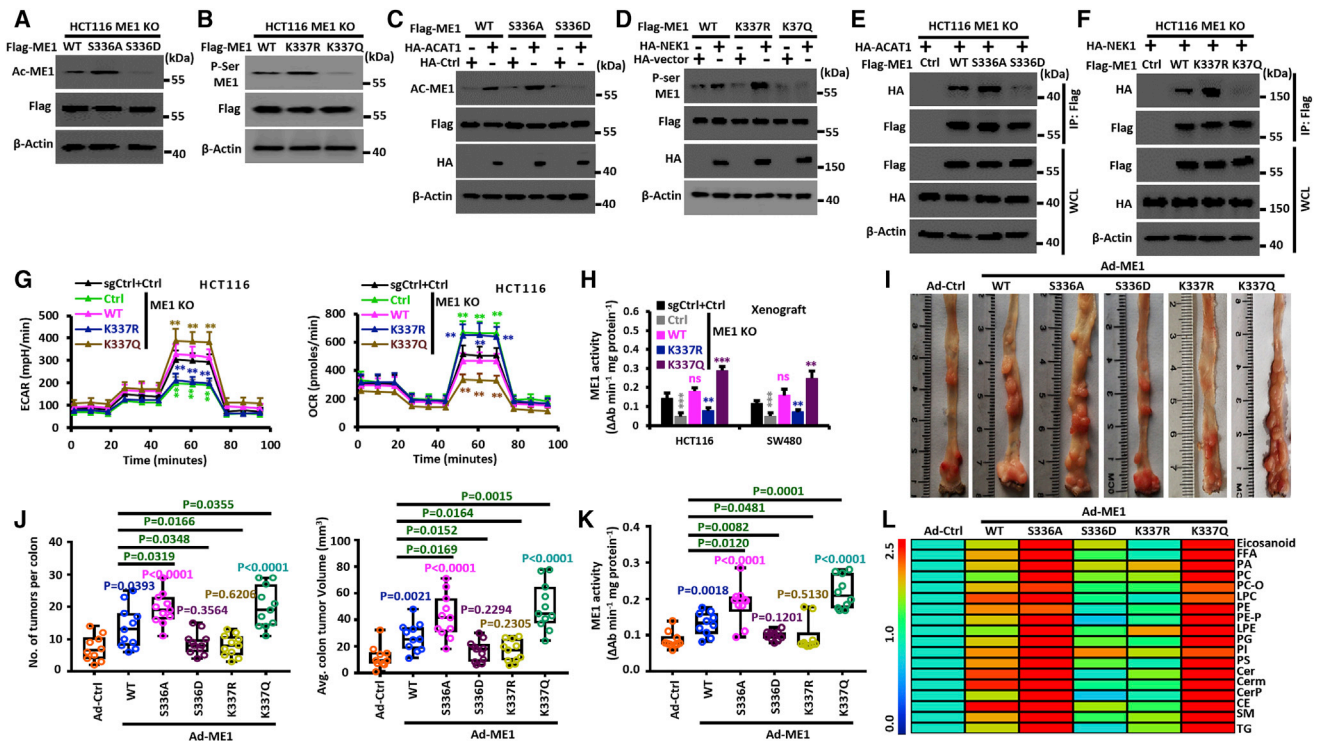
Figure 4. ME1 Acetylation and Phosphorylation Are Mutually Antagonistic

(A) Ectopic expression of ME1 S336A and S336D mutants increase and decrease its acetylation, respectively.

(B) Ectopic expression of ME1 S337R and S337Q mutant increase and decrease its serine phosphorylation, respectively.

(C) Ectopic ACAT1 expression promotes the acetylation of the ME1 S336A mutant but not the S336D mutant.

(D) Ectopic NEK1 expression increases the phosphorylation of the ME1 K337R mutant but not the K337Q mutant.

(E) ME1 mutants S336D and S336A, respectively inhibit and enhance the interaction between ACAT1 and ME1.

(F) ME1 K337R and K337Q mutants, respectively promote and inhibit the interaction with NEK1.

(G) ECAR (left) and OCR (right) analyses of ME1 acetylation site mutants in ME1-KO HCT116 cells.

(H) ME1 activity in lysates from indicated xenografts.

(I) Typical images of colon tumors expressing the indicated ME1 proteins 120 days after AOM/DSS treatment.

(J) Colon tumor numbers (left) and average tumor volume (right) in mice from (I).

(K) ME1 activity in CRCs of mice from (I).

Data were presented as mean ± SD. **p < 0.01, ***p < 0.001.

(L) Heatmap displays colon lipid species as detected via mass spectrometry. Scale bar represents fold change versus Ctrl. FFA, free fatty acids; PA, phospholipids alcohol; PC, phosphatidylcholine; PG, phosphatidyl glycerin; SM, sphingomyelin; Cer, ceramide; PS, phosphatidylserine; PI, phosphatidylinositol; CerP, ceramide phosphate; LPC, lyso-phosphatidylcholine; CE, cholesterol ester.

(J and K) Significance was performed using Wilcoxon signed rank test. The horizontal lines in the boxplots represent the median, the boxes represent the interquartile range, and the whiskers represent the minimal and maximal values.

ME1 K337 Acetylation Promotes CRC Growth

Next, we explored the biological consequences of ME1 K337 acetylation. Ectopic expression of ME1 acetylation mimicked K337Q but not K337R, significantly increased CRC *in vivo* growth, glycolysis, ME1 enzymatic activity, NADPH production, and lipid synthesis (Figures 4G, 4H, and S4B–S4H). These results demonstrate that ME1 K337 acetylation promotes CRC growth and metabolic re-programming.

ME1 S336 Dephosphorylation and K337 Acetylation Promotes AOM/DSS-Induced Colorectal Tumorigenesis in Mice

The AOM/DSS-induced CRC mouse model was used to evaluate the effects of post-translational modification of ME1 on colorectal tumorigenesis. C57/B6 mice were injected intra-peri-

toneally with AOM, followed by injections of DSS and adenoviral vectors encoding WT or mutant forms of ME1. Mice were sacrificed 120 days after AOM injection and ME1 expression was confirmed by western blot (Figures S4I and S4J). Compared to mice injected with a control adenoviral vector, those expressing WT ME1 developed more and larger CRCs (Figures 4I, 4J, and S4K) and showed high levels of NADPH production and lipid synthesis (Figures 4K, 4L, and S4L–S4T). In contrast, animals expressing the ME1 S336D and K337R mutants had similar tumor burdens and all previously identified activities (Figures 4I–4L and S4K–S4T). Unexpectedly, mice expressing the S336A and K337Q mutants developed more numerous and larger CRCs (Figures 4I, 4J, and S4K) and had higher levels of the above-described activities (Figures 4K, 4L, and S4L–S4T). These results reveal the critical and reciprocal roles of ME1 S336
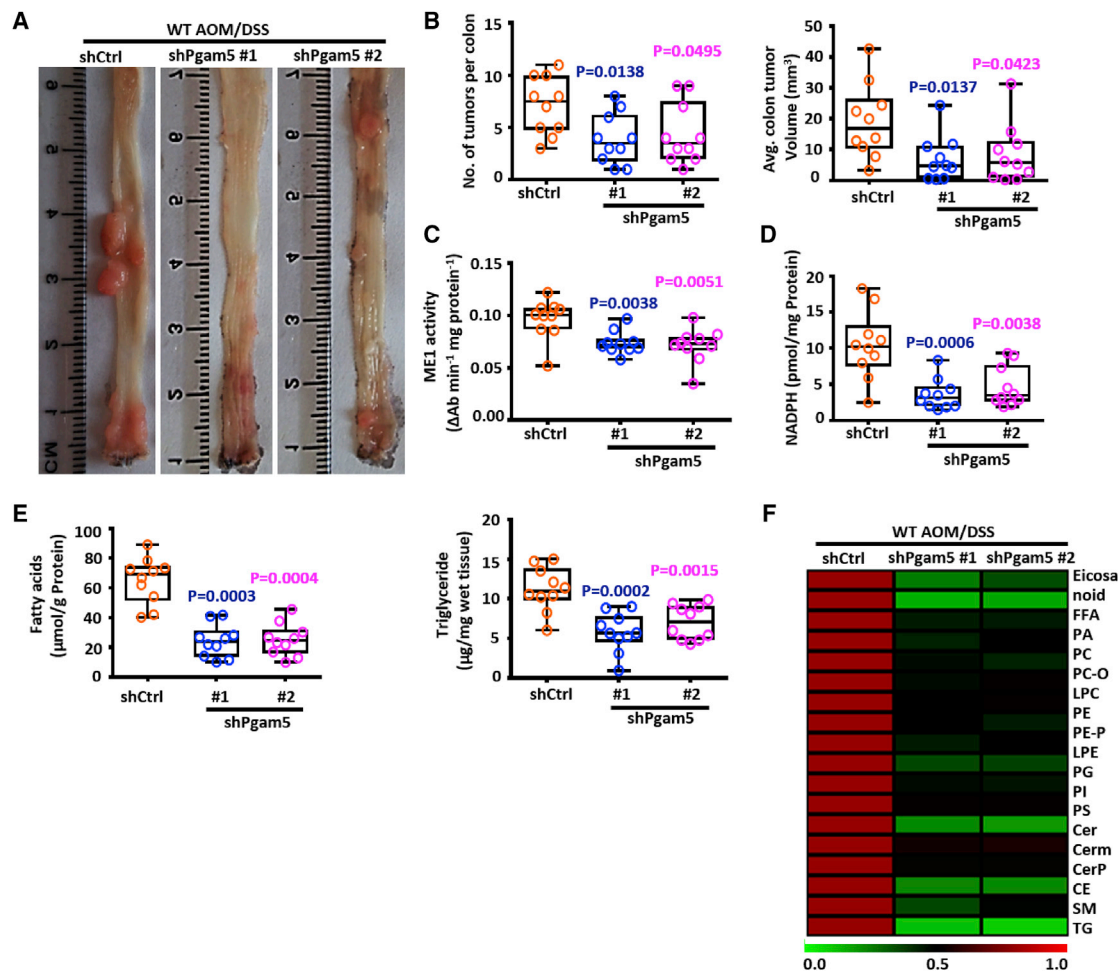
Figure 5. Depletion of PGAM5 Attenuates Chemically Induced CRC Tumorigenesis in Mice

(A) Typical images of colon tumors from adeno-shCtrl- and adeno-shPgam5-treated mice 120 days after AOM/DSS treatment.

(B) Colon tumor numbers (left) and average tumor volumes (right) in mice from (A).

(C) ME1 activities in CRCs of mice from (A).

(D and E) NADPH (D), FA (E, left), and TG (E, right) levels in CRCs of mice from (A).

(F) Heatmap showing tumor lipid species from adeno-shPgam5-treated mice 120 days after AOM/DSS treatment as detected via mass spectrometry. Scale bar represents fold change versus shCtrl.

Data were presented as mean ± SD.

dephosphorylation and K337 acetylation in CRC development and lipid metabolism in mice.

Depletion of PGAM5 Attenuated Spontaneous and Chemically Induced Colorectal Tumorigenesis in Mice

To test the therapeutic potential of manipulating PGAM5 *in vivo*, we asked whether abrogation of its expression would inhibit tumor growth in the CRC mouse model. Concentrated adenovirus encoding shPgam5 was delivered intraperitoneally into AOM/DSS-treated WT mice and tumor burdens were assessed on day 120. Depletion of PGAM5 was confirmed by immunoblot (Figure S5A). Compared with mice treated with a control adenoviruses (shCtrl), these animals showed a significantly reduced tumor burden throughout the colon and decreased tumor proliferation (Figures 5A, 5B, S5B, and S5C). Abrogation of PGAM5

also significantly reduced all previously identified activities (Figures 5C–5F and S5D–S5K).

Adenomatous polyposis coli (*APC*) is the most frequently mutated gene in sporadic CRC cancer in humans and is nearly always mutated in familial adenomatous polyposis coli (FAP). *Apc*[Min/+] mice contain a germline *Apc* mutation, which predisposes to spontaneous colonic and small intestinal polyposis and serves as a model for human FAP (Peuker et al., 2016). qRT-PCR and western blot experiments showed that PGAM5 expression was significantly increased in *Apc*[Min/+] mice (Figures 1F and 1G). To investigate the role of PGAM5 in spontaneous tumor development, we treated the *Apc*[Min/+] mice with shPgam5-encoding adenovirus. This dramatically suppressed spontaneous colorectal and small intestine tumorigenesis (Figures S5L–S5O) and reduced ME1-related activities (Figures
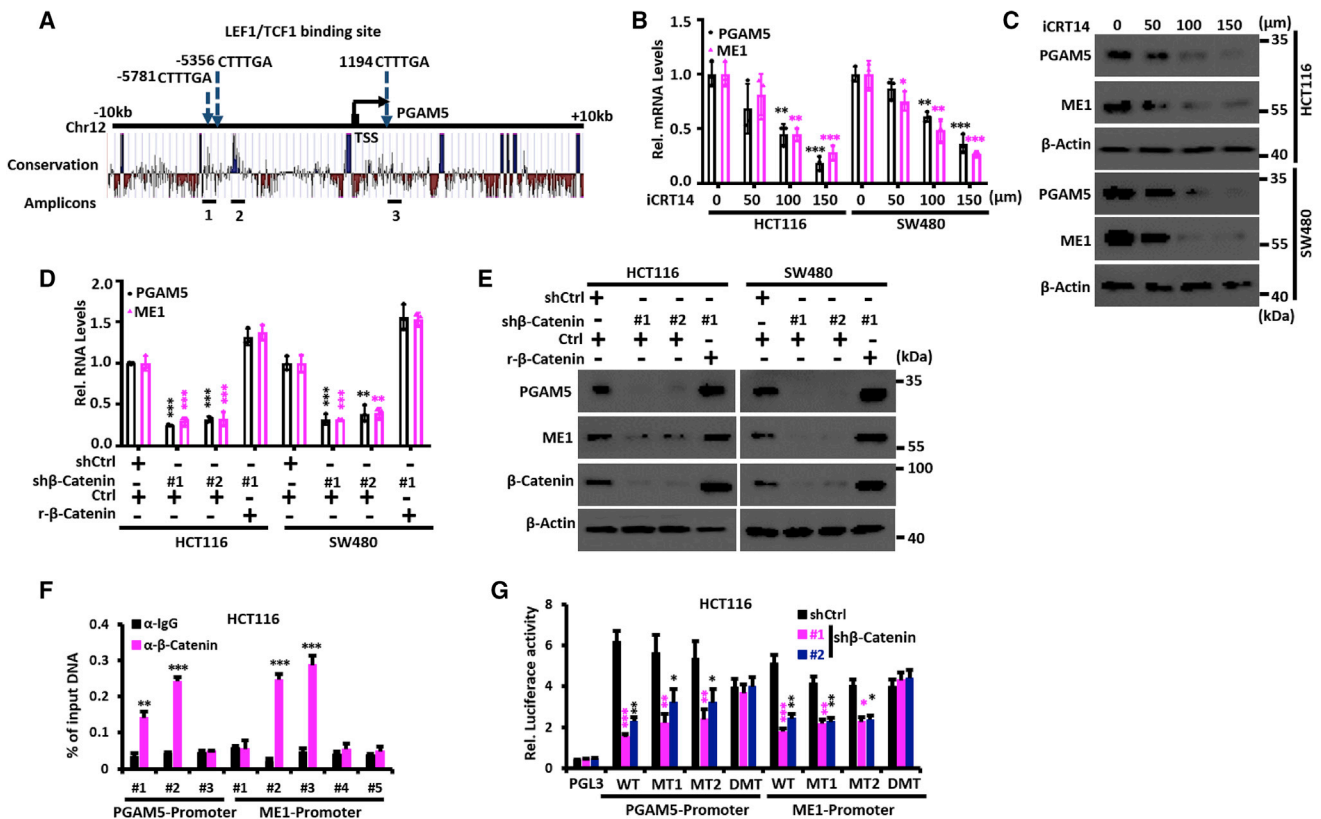
Figure 6. PGAM5 and ME1 Are Transcriptionally Activated by β-Catenin/TCF1

(A) Schematic diagram showing the location of LEF1/TCF1 binding sites in the *PGAM5* promoter from upstream −10 kb to downstream +10 kb. 1–3 are amplicons of CHIP-PCR. TSS, transcription start site.

(B) Dose-dependent inhibition of PGAM5 and ME1 mRNA levels by the LEF1/TCF1 inhibitor iCRT14 in HCT116 and SW480 cells.

(C) Dose-dependent inhibition of PGAM5 and ME1 protein by iCRT14 in HCT116 and SW480 cells.

(D and E) Relative mRNA (D) and protein levels (E) in HCT116 and SW480 CRC cells stably transfected with the indicated combinations of vectors.

(F) qPCR ChIP analyses of β-catenin binding to PGAM5 and ME1 promoter regions in HCT116 cells.

(G) Luciferase activity of different vectors in PGAM5 and ME1 promoter regions with β-catenin inhibition in HCT116 cells.

Data were presented as mean ± SD. *p < 0.05, **p < 0.01, ***p < 0.001.

S5P–S5T). Depletion of Pgam5 thus significantly inhibits tumor growth and lipid metabolism in both spontaneous and AOM/DSS-induced colorectal tumorigenesis in mice.

PGAM5 and ME1 Are Transcriptionally Activated by β-Catenin/TCF1 Complex

The previous bioinformatics results showed PGAM5 and ME1 to be dramatically upregulated in CRC (Figures S1D–S1F and S6A) but without evidence for gene amplification (Figures S6B and S6C). Because mutational activation of the APC/WNT/β-catenin signaling is pivotal during CRC development (Peuker et al., 2016), we tested whether WNT/β-catenin signaling was responsible for PGAM5 and ME1 overexpression in CRC. To this end, we analyzed the putative transcription factor binding sites within the PGAM5 and ME1 promoter regions (−10 to +10 kb) in the Motifmap website. TCF/LEF emerged as the top candidate and its candidate binding sites were largely conserved in PGAM5 and ME1 promoters (Figures 6A and S6D). Supporting the functional relevance of this, both PGAM5 and ME1 RNA and protein were highly downregulated following treatment of

CRC cells with iCRT14, a potent inhibitor of the β-catenin-TCF/LEF interaction (Figures 6B and 6C). Depletion of β-catenin had the similar effect (Figures 6D and 6E). Meanwhile, the protein levels of PGAM5, ME1, and acetylation of ME1 were dramatically increased, and NEK1 and phosphorylation of ME1 were decreased in NCM460 cells stimulated with Wnt3a (Figure S6E).

We next tested whether β-catenin directly transactivates PGAM5 and ME1, using chromatin immunoprecipitation (ChIP) assays. The results showed that β-catenin occupied the promoters of both PGAM5 and ME1 in HCT116 cells (Figures 6F and S6F). To confirm this, luciferase reporters containing PGAM5 and ME1 promoter elements were shown to be responsive to ectopic β-catenin expression. Moreover, short hairpin RNA (shRNA)-mediated β-catenin suppression dramatically decreased luciferase activity driven by WT promoters, but not by those with mutant β-catenin binding sites (Figures 6G and S6G). Thus, β-catenin activation facilitates tumor growth via the direct upregulation of PGAM5 and ME1 in CRC patients.
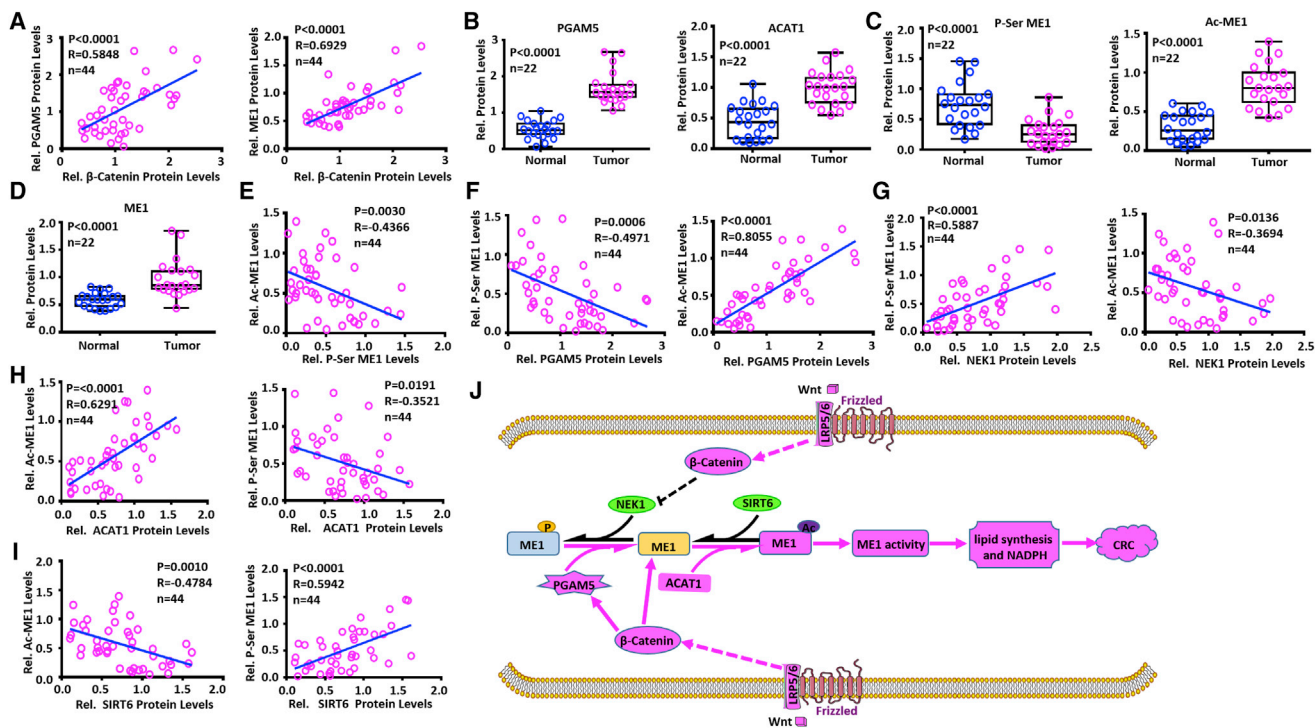
Figure 7. ME1 Acetylation and Phosphorylation are Up-regulated and Down-regulated Respectively in Human CRCs

(A) Correlation of PGAM5 (A, left) and ME1 (A, right) protein levels with β-catenin protein levels from CRC samples.

(B–D) Relative protein levels of PGAM5 (B, left), ACAT1 (B, right), P-Ser ME1 (C, left), Ac-ME1 (C, right), ME1 (D). The results shown are from the same tissues shown in Figure S7A.

(E) Correlation of Ac-ME1 protein levels with P-Ser ME1 protein levels from CRC samples.

(F) Correlation of P-Ser ME1 (F, left) and Ac-ME1 (F, right) protein levels with PGAM5 protein levels from CRC samples.

(G) Correlation of P-Ser ME1 (G, left) and Ac-ME1 (G, right) protein levels with NEK1 protein levels from CRC samples.

(H) Correlation of Ac-ME1 (H, left) and P-Ser ME1 (H, right) protein levels with ACAT1 protein levels from CRC samples.

(I) Correlation of Ac-ME1 (I, left) and P-Ser ME1 (I, right) protein levels with SIRT6 protein levels from CRC samples.

(A, E–I) Each circle is an individual sample. R, Spearman correlation coefficient.

(J) Schematic summary. β-catenin/TCF1 transcriptionally upregulates PGAM5 and ME1. PGAM5-mediated ME1 dephosphorylation and ACAT1-mediated ME1 acetylation increase ME1 activity to promote lipid metabolism and CRC development. Conversely, NEK1-mediated ME1 phosphorylation and SIRT6-mediated ME1 deacetylation repress these processes.

ME1 S336 Phosphorylation and K337 Acetylation Are Downregulated and Upregulated in Human CRC, Respectively

To investigate the clinical relevance of β-catenin, PGAM5, NEK1, ACAT1, SIRT6, phosphorylation, and acetylation of ME1, we collected 22 CRC samples (T) with adjacent normal colon tissues (N) and performed quantitative immunoblotting (Figure S7A). Our findings showed that β-catenin levels positively correlated with PGAM5 and ME1 in the above samples (Figure 7A). Both PGAM5 and ACAT1 proteins were also significantly increased in these CRC samples (Figure 7B), whereas NEK1 and SIRT6 were decreased (Figure S7B). ME1 phosphorylation was deceased whereas its acetylation and total levels were increased (Figures 7C and 7D). Overall, ME1 phosphorylation and acetylation were negatively correlated (Figure 7E), whereas PGAM5 was negatively correlated with phosphorylation and positively correlated with acetylation of ME1 (Figure 7F). NEK1 positively correlated with ME1 phosphorylation but negatively correlated with its acetylation and PGAM5 expression (Figures 7G and S7C).

ACAT1 was positively correlated with ME1 acetylation and negatively correlated with phosphorylation of ME1 (Figure 7H). Finally, SIRT6 was negatively correlated with acetylation of ME1 and ACAT1, but positively correlated with ME1 phosphorylation (Figures 7I and S7D). Collectively, these data are consistent with the proteomic and biochemical findings discussed above and support the idea that post-translational modification of ME1 plays a crucial role in human CRC development.

DISCUSSION

The regulation of signaling pathways by protein kinases and phosphatases is necessary to achieve well-coordinated and limited cellular outcomes in response to opposing environmental cues (Robitaille et al., 2013; Yang et al., 2012). In many cases, kinase/phosphatase complex signaling is both temporally and spatially dynamic in order to permit fine control over substrate phosphorylation status (Ben-Sahra et al., 2013; Fan et al., 2014; Gao et al., 2019). Such complexes may be necessary for

cancer development and can therefore be considered as potential therapeutic targets. Protein kinase inhibitors have long been used to treat a variety of tumors, including CRC, and in some cases have achieved remarkable therapeutic outcomes and survival benefits (Liao et al., 2017; Mason et al., 2017). In contrast, the clinical application of phosphatase inhibitors has been significantly more modest, thus presenting a significant therapeutic opportunity.

The current study reveals a molecular mechanism underlying ME1 regulation in highly proliferative CRC cells and suggests that targeting ME1's post-translational modifications represents a promising therapeutic strategy. Our findings point to the existence of a dynamic equilibrium between ME1 phosphorylation and acetylation, representing inactive and active forms, respectively (Figure 7J). In normal proliferating cells, such as those stimulated by WNT, ME1 is dephosphorylated by PGAM5 and acetylated by ACAT1, leading to active ME1 dimerization. Moreover, this mechanism may be hijacked in human cancer cells, where oncogenic WNT/β-catenin signaling is commonly upregulated. These results suggest a molecular mechanism by which metabolic enzymes are regulated via competing phosphorylation/acetylation reactions in response to normal and oncogenic signaling.

PGAM5 normally resides on the mitochondrial outer membrane and has been implicated in a variety of cellular activities related to the control of signal transduction pathways (He et al., 2017; Wang et al., 2012). PGAM5 has also been identified in the cytoplasm where it participates in the activation of WNT/β-catenin signaling (Bernkopf et al., 2018; Rauschenberger et al., 2017). This study indicates that PGAM5 dramatically enhances lipid metabolism and CRC growth through its direct interaction with and dephosphorylation of ME1 (Figure 7J). These results suggest that the targeting of PGAM5 phosphatase activity could be of therapeutic benefit in CRC and other cancers with high-level PGAM5 activity (Figure S1D).

The mutual acetylation and deacetylation of metabolic enzymes also play important roles in tumorigenesis (Fan et al., 2016; Lin et al., 2013), but their precise function in CRC development is largely unknown. In this study, we identified ACAT1 and SIRT6 as the ME1 acetylase and deacetylase, respectively. Recently ACAT1 has been reported to enhance tumor growth by increasing the acetylation of pyruvate dehydrogenase phosphatase 1 (PDP1) in a manner that is dependent upon Y381 phosphorylation status (Fan et al., 2014). The phosphorylation of ACAT1 itself on Y407 dramatically increases tumor growth by regulating its activity and tetramerization (Fan et al., 2016). SIRT6 plays a key role in regulating lipid metabolism and tumorigenesis. For example, SIRT6 promotes DNA repair and its loss leads to abnormalities in mice that overlap with aging-associated degenerative processes (Ghosh et al., 2018; Kugel et al., 2016). Meanwhile, SIRT6 deacetylates and significantly increases the activity of nicotinamide phosphoribosyltransferase (NAMPT). NAMPT is the rate-limiting enzyme of the NAD^+ salvage pathway and also plays important roles in aging (Sociali et al., 2019). Together with these findings, our results suggest that ACAT1 and SIRT6 regulate lipid metabolism and CRC tumorigenesis by dynamically regulating ME1 acetylation (Figure 7M). Therefore,

ACAT1 inhibitors and/or SIRT6 agonists also merit consideration for the treatment of CRC.

Reprogramming metabolism is a major hallmark of cancer (Hanahan and Weinberg, 2011). Altered lipid synthesis in particular plays an extremely critical role in tumor growth. In rapidly proliferating tumor cells, for example, a high level of lipid synthesis provides precursors for membrane biogenesis and steroid hormones. Many studies have shown that lipid uptake and *de novo* lipid synthesis are markedly increased in tumor cells (Cheng et al., 2017; Cotte et al., 2018). ME1 is an $NADP^+$-dependent enzyme that generates NADPH for fatty acid biosynthesis via the reversible oxidative decarboxylation of malate and the production of pyruvate, thereby linking glycolysis and the TCA cycle. ME1 upregulation has been observed in a wide spectrum of cancers, including gastric cancer, liver cancer, and CRC (Fernandes et al., 2018; Lu et al., 2018; Wen et al., 2015). In this study, we have demonstrated two inter-dependent post-translational modifications for ME1 by which S336 phosphorylation inhibits enzymatic activity by disrupting its ACAT1-dependent acetylation on the adjacent K337 residue and subsequent ME1 dimerization. In a reciprocal manner, K337 acetylation increases ME1 activity by blocking S336 phosphorylation and promoting dimerization (Figure 7M). Both S336 and K337 reside on the surface of ME1 (https://www.rcsb.org/3d-view/1PJ4/1), thus potentially allowing ready accessibility to each of the four post-translational modifying enzymes. ME1 interacts with PGAM5 and ACAT1 in mitochondria but not the cytosol. This indicates that ME1 shuttles between mitochondria and cytosol and might be regulated by different post-translational modifications in these compartments. Furthermore, the binding of phosphorylated ME1 to PGAM5 but not NEK1, and the binding of acetylated ME1 to SIRT6 but not ACAT1, suggests that phosphorylated but unacetylated ME1 is located to mitochondria whereas acetylated but unphosphorylated ME1 is located to the cytosol. Consistent with this, the results of our subcellular localization studies showed ME1 S336D and K337R to be mainly localized to mitochondria whereas S336A and K337Q were mainly cytosolic. Whether the binary and mutually exclusive choice between phosphorylation and acetylation of these two residues is based on steric hindrance, electrostatic repulsion, or some combination of the two remains to be determined as does whether either of the modifications of these residues leads to structural alterations that preclude alteration by the other modifying enzymes. In pigeons, ME1 S346, which corresponds to human ME1 S336, is reported to be necessary for binding $NADP^+$ (Chang and Tong, 2003). Once ME1 S336 is phosphorylated, the electronegativity of S336 is greatly enhanced, and the active center of acetylase is unable to bind K337 in the optimum conformation and orientation. As a result, the original hydrogen bond between ME1 and NADPH is interrupted, resulting in a greatly weakened bond between ME1 and $NADP^+$. As K337 acetylation increases, the hydrophobicity of ME1 weakening the binding of the kinase to adjacent S336 is enhanced as the active site of its kinase could not bind the substrate in the optimum conformation and orientation. As the hydrophobicity of the ME1 protein increases once its acetylation, the possibility of dimer turning over into tetramer may increase. Such questions can likely be resolved by further structural studies.

Reciprocal S336 phosphorylation and K337 acetylation regulate NAPDH production and lipid synthesis largely by affecting ME1 activity. These findings indicated that post-translational modifications of ME1 are likely to be dynamic and thus subject to significant change during the course of tumor development and/or in response to environmental changes that temporarily favor tumor growth or quiescence. Small molecule inhibitors that impair ME1 acetylation and/or dephosphorylation may thus represent viable future strategies for the treatment of CRC.

STAR★METHODS

Detailed methods are provided in the online version of this paper and include the following:

- KEY RESOURCES TABLE
- LEAD CONTACT AND MATERIALS AVAILABILITY
- EXPERIMENTAL MODEL AND SUBJECT DETAILS
  - ○ Cell Culture and Stable Cell Lines
  - ○ Human CRC Samples
- METHOD DETAILS
  - ○ Plasmids and Constructs
  - ○ Co-IP and Immunoblot
  - ○ Metabolic Assays
  - ○ Extracellular Acidification Rate (ECAR) and Oxygen Consumption Rate (OCR) Assays
  - ○ ROS Detection in Intracellular and Tumor Tissues
  - ○ Reporter, CHIP, and qPCR Assays
  - ○ Animal Experiments
  - ○ IHC Assays
  - ○ Lipidomics Assays
  - ○ Bioinformatic Analysis
- QUANTIFICATION AND STATISTICAL ANALYSIS
- DATA AND CODE AVAILABILITY

SUPPLEMENTAL INFORMATION

Supplemental Information can be found online at https://doi.org/10.1016/j.molcel.2019.10.015.

AUTHOR CONTRIBUTIONS

Y.Z. and Y.L. designed the study. Y.Z. and L.G. performed most of the experiments. X.L. constructed plasmids. K.C. performed bioinformatics analyses. C.L. and B.L. performed some animal experiments. F.Z. and Q.Z. provided reagents and clinical assistance. E.V.P. and C.F. provided reagents and conceptual advice. All authors discussed the results. Y.Z., E.P., and Y.L. wrote the manuscript with comments from all authors.

DECLARATION OF INTERESTS

The authors declare no competing interests.

REFERENCES

Ben-Sahra, I., Howell, J.J., Asara, J.M., and Manning, B.D. (2013). Stimulation of de novo pyrimidine synthesis by growth signaling through mTOR and S6K1. Science *339*, 1323–1328.

Bernkopf, D.B., Jalal, K., Brückner, M., Knaup, K.X., Gentzel, M., Schambony, A., and Behrens, J. (2018). Pgam5 released from damaged mitochondria induces mitochondrial biogenesis via Wnt signaling. J. Cell Biol. *217*, 1383–1394.

Chang, G.G., and Tong, L. (2003). Structure and function of malic enzymes, a new class of oxidative decarboxylases. Biochemistry *42*, 12721–12733.

Cheng, J., Qian, D., Ding, X., Song, T., Cai, M., Dan Xie, Wang, Y., Zhao, J., Liu, Z., Wu, Z., et al. (2018). High PGAM5 expression induces chemoresistance by enhancing Bcl-xL-mediated anti-apoptotic signaling and predicts poor prognosis in hepatocellular carcinoma patients. Cell Death Dis. *9*, 991.

Cheng, L., Zhu, Y., Han, H., Zhang, Q., Cui, K., Shen, H., Zhang, J., Yan, J., Prochownik, E., and Li, Y. (2017). MicroRNA-148a deficiency promotes hepatic lipid metabolism and hepatocarcinogenesis in mice. Cell Death Dis. *8*, e2916.

Cotte, A.K., Aires, V., Fredon, M., Limagne, E., Derangère, V., Thibaudin, M., Humblin, E., Scagliarini, A., de Barros, J.P., Hillon, P., et al. (2018). Lysophosphatidylcholine acyltransferase 2-mediated lipid droplet production supports colorectal cancer chemoresistance. Nat. Commun. *9*, 322.

Dey, P., Baddour, J., Muller, F., Wu, C.C., Wang, H., Liao, W.T., Lan, Z., Chen, A., Gutschner, T., Kang, Y., et al. (2017). Genomic deletion of malic enzyme 2 confers collateral lethality in pancreatic cancer. Nature *542*, 119–123.

Fan, J., Shan, C., Kang, H.B., Elf, S., Xie, J., Tucker, M., Gu, T.L., Aguiar, M., Lonning, S., Chen, H., et al. (2014). Tyr phosphorylation of PDP1 toggles recruitment between ACAT1 and SIRT3 to regulate the pyruvate dehydrogenase complex. Mol. Cell *53*, 534–548.

Fan, J., Lin, R., Xia, S., Chen, D., Elf, S.E., Liu, S., Pan, Y., Xu, H., Qian, Z., Wang, M., et al. (2016). Tetrameric Acetyl-CoA Acetyltransferase 1 Is Important for Tumor Growth. Mol. Cell *64*, 859–874.

Fernandes, L.M., Al-Dwairi, A., Simmen, R.C.M., Marji, M., Brown, D.M., Jewell, S.W., and Simmen, F.A. (2018). Malic Enzyme 1 (ME1) is pro-oncogenic in *Apc*^Min/+ mice. Sci. Rep. *8*, 14268.

Finicle, B.T., Jayashankar, V., and Edinger, A.L. (2018). Nutrient scavenging in cancer. Nat. Rev. Cancer *18*, 619–633.

Gao, T., Li, M., Mu, G., Hou, T., Zhu, W.G., and Yang, Y. (2019). PKCζ Phosphorylates SIRT6 to Mediate Fatty Acid β-Oxidation in Colon Cancer Cells. Neoplasia *21*, 61–73.

Ghosh, S., Wong, S.K., Jiang, Z., Liu, B., Wang, Y., Hao, Q., Gorbunova, V., Liu, X., and Zhou, Z. (2018). Haploinsufficiency of *Trp53* dramatically extends the lifespan of Sirt6-deficient mice. eLife *7*, e32127.

Gu, L., Zhu, Y., Lin, X., Li, Y., Cui, K., Prochownik, E.V., and Li, Y. (2018). Amplification of Glyceronephosphate O-Acyltransferase and Recruitment of USP30 Stabilize DRP1 to Promote Hepatocarcinogenesis. Cancer Res. *78*, 5808–5819.

Hanahan, D., and Weinberg, R.A. (2011). Hallmarks of cancer: the next generation. Cell *144*, 646–674.

Hao, Y., Samuels, Y., Li, Q., Krokowski, D., Guan, B.J., Wang, C., Jin, Z., Dong, B., Cao, B., Feng, X., et al. (2016). Oncogenic PIK3CA mutations reprogram glutamine metabolism in colorectal cancer. Nat. Commun. *7*, 11971.

He, G.W., Günther, C., Kremer, A.E., Thonn, V., Amann, K., Poremba, C., Neurath, M.F., Wirtz, S., and Becker, C. (2017). PGAM5-mediated programmed necrosis of hepatocytes drives acute liver injury. Gut *66*, 716–723.

Jiang, P., Du, W., Mancuso, A., Wellen, K.E., and Yang, X. (2013). Reciprocal regulation of p53 and malic enzymes modulates metabolism and senescence. Nature 493, 689–693.

Kugel, S., Sebastián, C., Fitamant, J., Ross, K.N., Saha, S.K., Jain, E., Gladden, A., Arora, K.S., Kato, Y., Rivera, M.N., et al. (2016). SIRT6 Suppresses Pancreatic Cancer through Control of Lin28b. Cell 165, 1401–1415.

Liao, S., Davoli, T., Leng, Y., Li, M.Z., Xu, Q., and Elledge, S.J. (2017). A genetic interaction analysis identifies cancer drivers that modify EGFR dependency. Genes Dev. 31, 184–196.

Lin, R., Tao, R., Gao, X., Li, T., Zhou, X., Guan, K.L., Xiong, Y., and Lei, Q.Y. (2013). Acetylation stabilizes ATP-citrate lyase to promote lipid biosynthesis and tumor growth. Mol. Cell 51, 506–518.

Lu, Y.X., Ju, H.Q., Liu, Z.X., Chen, D.L., Wang, Y., Zhao, Q., Wu, Q.N., Zeng, Z.L., Qiu, H.B., Hu, P.S., et al. (2018). ME1 Regulates NADPH Homeostasis to Promote Gastric Cancer Growth and Metastasis. Cancer Res. 78, 1972–1985.

Makinoshima, H., Umemura, S., Suzuki, A., Nakanishi, H., Maruyama, A., Udagawa, H., Mimaki, S., Matsumoto, S., Niho, S., Ishii, G., et al. (2018). Metabolic Determinants of Sensitivity to Phosphatidylinositol 3-Kinase Pathway Inhibitor in Small-Cell Lung Carcinoma. Cancer Res. 78, 2179–2190.

Mason, J.M., Wei, X., Fletcher, G.C., Kiarash, R., Brokx, R., Hodgson, R., Beletskaya, I., Bray, M.R., and Mak, T.W. (2017). Functional characterization of CFI-402257, a potent and selective Mps1/TTK kinase inhibitor, for the treatment of cancer. Proc. Natl. Acad. Sci. USA 114, 3127–3132.

Panda, S., Srivastava, S., Li, Z., Vaeth, M., Fuhs, S.R., Hunter, T., and Skolnik, E.Y. (2016). Identification of PGAM5 as a Mammalian Protein Histidine Phosphatase that Plays a Central Role to Negatively Regulate CD4(+) T Cells. Mol. Cell 63, 457–469.

Peuker, K., Muff, S., Wang, J., Künzel, S., Bosse, E., Zeissig, Y., Luzzi, G., Basic, M., Strigli, A., Ulbricht, A., et al. (2016). Epithelial calcineurin controls microbiota-dependent intestinal tumor development. Nat. Med. 22, 506–515.

Qi, X.M., Wang, F., Mortensen, M., Wertz, R., and Chen, G. (2018). Targeting an oncogenic kinase/phosphatase signaling network for cancer therapy. Acta. Pharm. Sin. B. 8, 511–517.

Qian, H., Chen, Y., Nian, Z., Su, L., Yu, H., Chen, F.J., Zhang, X., Xu, W., Zhou, L., Liu, J., et al. (2017). HDAC6-mediated acetylation of lipid droplet-binding protein CIDEC regulates fat-induced lipid storage. J. Clin. Invest. 127, 1353–1369.

Ramachandran, A., and Jaeschke, H. (2017). PGAM5: a new player in immune-mediated liver injury. Gut 66, 567–568.

Rauschenberger, V., Bernkopf, D.B., Krenn, S., Jalal, K., Heller, J., Behrens, J., Gentzel, M., and Schambony, A. (2017). The phosphatase Pgam5 antagonizes Wnt/β-Catenin signaling in embryonic anterior-posterior axis patterning. Development 144, 2234–2247.

Robitaille, A.M., Christen, S., Shimobayashi, M., Cornu, M., Fava, L.L., Moes, S., Prescianotto-Baschong, C., Sauer, U., Jenoe, P., and Hall, M.N. (2013). Quantitative phosphoproteomics reveal mTORC1 activates de novo pyrimidine synthesis. Science 339, 1320–1323.

Shan, C., Kang, H.B., Elf, S., Xie, J., Gu, T.L., Aguiar, M., Lonning, S., Hitosugi, T., Chung, T.W., Arellano, M., et al. (2014). Tyr-94 phosphorylation inhibits pyruvate dehydrogenase phosphatase 1 and promotes tumor growth. J. Biol. Chem. 289, 21413–21422.

Shen, H., Xing, C., Cui, K., Li, Y., Zhang, J., Du, R., Zhang, X., and Li, Y. (2017). MicroRNA-30a attenuates mutant KRAS-driven colorectal tumorigenesis via direct suppression of ME1. Cell Death Differ. 24, 1253–1262.

Sociali, G., Grozio, A., Caffa, I., Schuster, S., Becherini, P., Damonte, P., Sturla, L., Fresia, C., Passalacqua, M., Mazzola, F., et al. (2019). SIRT6 deacetylase activity regulates NAMPT activity and NAD(P)(H) pools in cancer cells. FASEB J. 33, 3704–3717.

Torre, L.A., Bray, F., Siegel, R.L., Ferlay, J., Lortet-Tieulent, J., and Jemal, A. (2015). Global cancer statistics, 2012. CA Cancer J. Clin. 65, 87–108.

Wang, Z., Jiang, H., Chen, S., Du, F., and Wang, X. (2012). The mitochondrial phosphatase PGAM5 functions at the convergence point of multiple necrotic death pathways. Cell 148, 228–243.

Wen, D., Liu, D., Tang, J., Dong, L., Liu, Y., Tao, Z., Wan, J., Gao, D., Wang, L., Sun, H., et al. (2015). Malic enzyme 1 induces epithelial-mesenchymal transition and indicates poor prognosis in hepatocellular carcinoma. Tumour Biol. 36, 6211–6221.

Yang, W., Zheng, Y., Xia, Y., Ji, H., Chen, X., Guo, F., Lyssiotis, C.A., Aldape, K., Cantley, L.C., and Lu, Z. (2012). ERK1/2-dependent phosphorylation and nuclear translocation of PKM2 promotes the Warburg effect. Nat. Cell Biol. 14, 1295–1304.

Zadra, G., Ribeiro, C.F., Chetta, P., Ho, Y., Cacciatore, S., Gao, X., Syamala, S., Bango, C., Photopoulos, C., Huang, Y., et al. (2019). Inhibition of de novo lipogenesis targets androgen receptor signaling in castration-resistant prostate cancer. Proc. Natl. Acad. Sci. USA 116, 631–640.

Zhu, Y., Gu, L., Li, Y., Lin, X., Shen, H., Cui, K., Chen, L., Zhou, F., Zhao, Q., Zhang, J., et al. (2017). miR-148a inhibits colitis and colitis-associated tumorigenesis in mice. Cell Death Differ. 24, 2199–2209.